Analysis of Reassignment Operators Used in Synchrosqueezing Transforms: With an Application to Instantaneous Frequency Estimation

Sylvain Meignen, Neha Singh

Analysis of Reassignment Operators Used in Synchrosqueezing Transforms: With an Application to Instantaneous Frequency Estimation

Sylvain Meignen and Neha Singh

***Abstract*—In this paper, our goal is to investigate the behavior of reassignment operators used in synchrosqueezing transforms to reassign the time-frequency representation of multicomponent signals made of the superposition of amplitude and frequency modulated modes. Indeed, while these operators are particularly efficient on specific types of modes, their quality worsens drastically when the modes depart from the ideal case they are designed for. In particular, when these interfere in the time-frequency plane or when some noise is present, we show the limits to the use of these reassignment operators for the estimation of the instantaneous frequency of the modes by studying their behavior in the vicinity of spectrogram ridges, and then propose a novel approach to circumvent these limitations.**

***Index Terms*—time-frequency analysis, Fourier-based synchrosqueezing, reassignment methods**

I. Introduction

MULTICOMPONENT signals (MCSs) are very often used to represent non-stationary signals encountered in many different fields such as pathology diagnosis [1], [2], structural damage [3], [4] or physiological signals [5]. To analyze this type of signals the *short-time Fourier transform* (STFT) is very often considered since, with that *time-frequency representation* (TFR), the modes making up a MCS are associated with specific regions around *ridges* in the time-frequency (TF) plane [6], which consist of *instantaneous frequency* (IF) estimators of the modes [7], [8]. In that context, the IF estimates correspond to some specific local extrema along the frequency axis of the spectrogram. Other IF estimators can be designed by considering the reassignment operators used in *synchrosqueezing transforms* (SSTs), which can be applied to STFT [9], [10], to obtain the so-called *Fourier-based synchrosqueezing transform* (FSST), or to the continuous wavelet transform [11], [12]. SSTs have been widely used in various domains of applications among which fault diagnosis [13], [14], analysis of seismic signals [15], medical data analysis [5], [16], [17] and characterization of voice jitter [18] to name a few.

Variants of FSST were proposed to take into account the different nature of the modes to be reassigned. Indeed, in the seminal work of [9], [10] FSST used an IF estimator proved to be very accurate only when the modes can be locally approximated by pure harmonic modes. This approach was then extended by considering local linear chirp approximation for the modes in [19], [20], and then by assuming the modes have higher degree polynomial phases [21].

Nevertheless, the quality of the IF estimators used in FSSTs strongly depends on how well the modes are separated in the TF plane and also on the presence of noise. In particular, these estimates are ill-defined when the modes are crossing in the TF plane and a separation condition is assumed on the modes. It is worth noting here that recent works have tried to deal with crossing modes by estimating the chirp rate and IF simultaneously [22], while many different techniques have been developed to improve the separation of the modes by considering so-called *adaptive STFT* [23]–[26].

However, to adapt the window length in STFT as is done in adaptive STFT does not warranty perfect IF estimation in noisy situations, and windows with different lengths at each time are to be used to estimate the IF of the different modes [24]. When only one window is used, the optimal window length is often computed using the properties of the Rényi entropy [27], [28], which is proved to lead to optimal concentration measure in the case of a linear chirp [29].

As to improve IF estimation of the modes by only modifying the window length is somewhat limited, we here propose to focus on the study of the IF estimators used in FSSTs in the case of interference or noise. In a first section, we introduce the notations that are used throughout the paper, and then recall the definition of the IF estimators used in FSSTs, which take simpler forms when the window is the Gaussian window. In the next section, we recall the relation between these IF estimators and reassignment vectors, whose zeros are shown to satisfy simple equations. We then propose different new expressions to approximate reassignment vectors in the vicinity of their zeros, this being done to better analyze what is at work in the reassignment processes on the specific examples that we study next. Indeed, in the next section, we investigate the behavior of reassignment vectors on interfering modes, and propose a novel technique to compute the IF of the modes, while the last section does the same but this time for noisy mono-component signals.

II. Notations

A. Short-Time Fourier Transform

In this section, we introduce a series of definitions that will be used throughout the paper. Considering a signal $f \in$

The authors are with the Jean Kuntzmann Laboratory, University Grenoble Alpes and CNRS 5225, Grenoble 38401, France (emails: nehairo.iitr@gmail.com, sylvain.meignen@univ-grenoble-alpes.fr). This work was supported in part by the University Grenoble Alpes under IRS Grant "AMUSETE" and the ANR ASCETE project with grant number ANR-19-CE48-0001-01.

$L^1(\mathbb{R}) \cap L^2(\mathbb{R})$ and a real window $h \in L^\infty(\mathbb{R}) \cap L^2(\mathbb{R})$, the (modified) Short-Time Fourier Transform (STFT) is defined as:

$$V_f^h(t,\eta) = \int_{\mathbb{R}} f(\tau) h(\tau - t) e^{-2i\pi(\tau - t)\eta} d\tau. \quad (1)$$

In the sequel, we are going to study multicomponent signals (MCSs), defined as the superposition of several AM-FM components as follows:

$$f(t) = \sum_{p=1}^{P} A_p(t) e^{2i\pi\phi_p(t)}, \quad (2)$$

in which we assume A_p is positive, and $\phi_p'(t) > 0$ such that $\phi_{p+1}'(t) > \phi_p'(t)$ where $\phi_p'(t)$ denotes the instantaneous frequency (IF) of mode f_p at time t.

B. Instantaneous Frequency Estimators Used in Synchrosqueezing Transforms

The IF of each mode of f can be estimated from STFT by defining a so-called *local instantaneous frequency* (LIF) estimator. This estimator used in *STFT-based synchrosqueezing transform* (FSST), is defined wherever $V_f^h(t,\eta) \neq 0$ by first considering the complex estimate:

$$\tilde{\omega}_f(t,\eta) = \frac{\partial_t V_f^h(t,\eta)}{2i\pi V_f^h(t,\eta)} = \eta - \frac{1}{2i\pi} \frac{V_f^{h'}(t,\eta)}{V_f^h(t,\eta)}, \quad (3)$$

the LIF estimator being then defined as

$$\widehat{\omega}_f(t,\eta) = \Re\left\{\tilde{\omega}_f(t,\eta)\right\} = \eta - \Re\left\{\frac{1}{2i\pi} \frac{V_f^{h'}(t,\eta)}{V_f^h(t,\eta)}\right\}. \quad (4)$$

The *Fourier based synchrosqueezing transform* (FSST) then consists of reassigning the STFT through:

$$T_f^h(t,\omega) = \int_{|V_f^h(t,\eta)|>\gamma} V_f^h(t,\eta) \delta(\omega - \widehat{\omega}_f(t,\eta)) d\eta, \quad (5)$$

where δ is the Dirac distribution and γ some threshold.

The quality of LIF estimator $\widehat{\omega}_f$ is however only satisfactory when the signal is made of perturbed purely harmonic modes. To overcome this limitation, a new LIF estimator was introduced based on a local linear chirp approximation [19], [20] and then used in the definition of *second-order STFT-based synchrosqueezing transform* (FSST2). More precisely, introducing the complex *time delay*:

$$\tilde{t}_f(t,\eta) = t - \frac{\partial_\eta V_f^h(t,\eta)}{2i\pi V_f^h(t,\eta)} = t + \frac{V_f^{th}(t,\eta)}{V_f^h(t,\eta)}, \quad (6)$$

and the *complex frequency modulation operator* [21] (we omit (t,η) for the sake of simplicity):

$$\tilde{q}_f = \frac{\partial_\eta \tilde{\omega}_f}{\partial_\eta \tilde{t}_f} = \frac{1}{2i\pi} \frac{V_f^{h'} V_f^{th} - V_f^h V_f^{th'} - \left(V_f^h\right)^2}{V_f^h V_f^{t^2 h} - \left(V_f^{th}\right)^2}, \quad (7)$$

the second-order complex LIF estimator is then defined by:

$$\tilde{\omega}_f^{[2]} = \begin{cases} \tilde{\omega}_f + \tilde{q}_f \times (t - \tilde{t}_f) \text{ if } \partial_\eta \tilde{t}_f \neq 0 \\ \tilde{\omega}_f \text{ otherwise,} \end{cases} \quad (8)$$

and $\widehat{\omega}_f^{[2]} = \Re\left\{\tilde{\omega}_f^{[2]}\right\}$ is the new LIF estimator. FSST2 is then defined by replacing $\widehat{\omega}_f$ by $\widehat{\omega}_f^{[2]}$ in (5).

New LIF estimators were then proposed to handle MCSs containing AM-FM modes having non-negligible $\phi_p^{(k)}(t)$ for $k \geq 3$, especially those with fast oscillating phase [21]. In a nutshell, let us consider $f(\tau) = A(\tau) e^{i2\pi\phi(\tau)}$ with $A(\tau)$ (*resp.* $\phi(\tau)$) equal to its S^{th}-order (*resp.* N^{th}-order) Taylor expansion for τ close to t, with $S \leq N$, meaning:

$$f(\tau) = \exp\left(\sum_{j=0}^{N} \frac{\left([\log(A_p)]^{(j)}(t) + i2\pi\phi_p^{(j)}(t)\right)(\tau - t)^j}{j!}\right). \quad (9)$$

From (9), and the definition of STFT we may write:

$$\begin{aligned} \partial_t V_f^h(t,\eta) = & \left([\log(A)]'(t) + 2i\pi\phi'(t)\right) V_f^h(t,\eta) \\ & + \sum_{j=2}^{N} r_j^{[N]}(t) V_f^{t^{j-1}h}(t,\eta) \\ = & \; r_1^{[N]}(t) V_f^h(t,\eta) + \sum_{j=2}^{N} r_j^{[N]}(t) V_f^{t^{j-1}h}(t,\eta) \end{aligned} \quad (10)$$

where $r_j^{[N]}(t) = \frac{[\log(A)]^{(j)}(t) + 2i\pi\phi^{(j)}(t)}{(j-1)!}$.

Now, when f is a multicomponent signal made of modes following (9), the equality (10) turns into an approximation, namely for (t,η) in the vicinity of $(t,\phi_p'(t))$ for some p, one may write:

$$\begin{aligned} & \partial_t V_f^h(t,\eta) \\ & = r_1^{[N]}(t,\eta) V_f^h(t,\eta) + \sum_{j=2}^{N} r_j^{[N]}(t,\eta) V_f^{t^{j-1}h}(t,\eta), \end{aligned} \quad (11)$$

where $r_j^{[N]}(t,\eta) \approx \frac{[\log(A_p)]^{(j)}(t) + 2i\pi\phi_p^{(j)}(t)}{(j-1)!}$, and $\Re\left\{\frac{r_1^{[N]}(t,\eta)}{2i\pi}\right\}$ thus approximates the IF of f_p. Defining $\tilde{\omega}_f^{[N]}(t,\eta) := \frac{r_1^{[N]}(t,\eta)}{2i\pi}$, we may write, when $V_f^h(t,\eta) \neq 0$, that [21]:

$$\tilde{\omega}_f^{[N]}(t,\eta) = \tilde{\omega}_f(t,\eta) - \sum_{j=2}^{N} r_j^{[N]}(t,\eta) \frac{V_f^{t^{j-1}h}(t,\eta)}{2i\pi V_f^h(t,\eta)}, \quad (12)$$

and then the LIF estimator corresponds to $\widehat{\omega}_f^{[N]}(t,\eta) := \Re\left\{\tilde{\omega}_f^{[N]}(t,\eta)\right\}$. A simple way to compute $r_1^{[N]}$ is to come back to Eq. (11) which, remarking that $\partial_\eta V_f^h(t,\eta) = -2i\pi V_f^{th}(t,\eta)$, can be written under the matrix form:

$$\begin{aligned} & \begin{bmatrix} \partial_t V_f^h \\ \frac{i}{2\pi}\partial_\eta\partial_t V_f^h \\ \vdots \\ \frac{i^{N-1}}{(2\pi)^{N-1}}\partial_\eta^{N-1}\partial_t V_f^h \end{bmatrix} \\ & = \begin{bmatrix} V_f^h & V_f^{th} & \cdots & V_f^{t^{N-1}h} \\ V_f^{th} & V_f^{t^2 h} & \cdots & V_f^{t^N h} \\ \vdots & \vdots & \ddots & \vdots \\ V_f^{t^{N-1}h} & V_f^{t^N h} & \cdots & V_f^{t^{2(N-1)}h} \end{bmatrix} \begin{bmatrix} r_1^{[N]} \\ r_2^{[N]} \\ \vdots \\ r_N^{[N]} \end{bmatrix} = DR. \end{aligned} \quad (13)$$

Based on simple properties of the determinant of matrices, one obtains that:

$$r_1^{[N]} = \frac{det(M_1)}{det(D)}, \tag{14}$$

with

$$M_1 = \begin{bmatrix} \partial_t V_f^h & V_f^{th} & \cdots & V_f^{t^{N-1}h} \\ \frac{i}{2\pi}\partial_\eta\partial_t V_f^h & V_f^{t^2h} & \cdots & V_f^{t^Nh} \\ \vdots & \vdots & \ddots & \vdots \\ \frac{i^{N-1}}{(2\pi)^{N-1}}\partial_\eta^{N-1}\partial_t V_f^h & V_f^{t^Nh} & \cdots & V_f^{t^{2(N-1)}h} \end{bmatrix}. \tag{15}$$

Then, as $\partial_t V_f^h = i2\pi\eta V_f^h - V_f^{g'}$, we get, for any $k \geq 1$:

$$\partial_\eta^k \partial_t V_f^h = (-2i\pi)^k \left(-kV_f^{t^{k-1}h} - V_f^{t^kh'} + 2i\pi\eta V_f^{t^kh}\right), \tag{16}$$

leading to: $det(M_1) = i2\pi\eta det(D) - det(U_1) - det(V_1)$ with:

$$U_1 = \begin{bmatrix} 0 & V_f^{th} & \cdots & V_f^{t^{N-1}h} \\ V_f^h & V_f^{t^2h} & \cdots & V_f^{t^Nh} \\ \vdots & \vdots & \ddots & \vdots \\ (N-1)V_f^{t^{N-2}h} & V_f^{t^Nh} & \cdots & V_f^{t^{2(N-1)}h} \end{bmatrix}, \tag{17}$$

$$V_1 = \begin{bmatrix} V_f^{h'} & V_f^{th} & \cdots & V_f^{t^{N-1}h} \\ V_f^{th'} & V_f^{t^2h} & \cdots & V_f^{t^Nh} \\ \vdots & \vdots & \ddots & \vdots \\ V_f^{t^{N-1}h'} & V_f^{t^Nh} & \cdots & V_f^{t^{2(N-1)}h} \end{bmatrix},$$

and thus

$$\widehat{\omega}_f^{[N]} = \frac{1}{2\pi}\Im\left\{r_1^{[N]}\right\} = \eta - \frac{1}{2\pi}\Im\left\{\frac{det(U_1) + det(V_1)}{det(D)}\right\} \tag{18}$$

C. Simplified IF Estimators when h is the Gaussian Window

When h is the Gaussian window $e^{-\pi\frac{t^2}{\sigma^2}}$, the LIF estimators introduced above have simpler expressions. Indeed, as $h'(t) = -\frac{2\pi}{\sigma^2}th(t)$, we have:

$$\widehat{\omega}_f = \eta + \Im\left\{\frac{1}{\sigma^2}\frac{V_f^{th}}{V_f^h}\right\}, \tag{19}$$

and we may rewrite $\widehat{\omega}_f^{[2]}$ as:

$$\begin{aligned} \widehat{\omega}_f^{[2]} &= \widehat{\omega}_f + \Re\left\{\frac{1}{2i\pi}\frac{(V_f^h)^2 + V_f^hV_f^{th'} - V_f^{h'}V_f^{th}}{V_f^hV_f^{t^2h} - (V_f^{th})^2}\frac{V_f^{th}}{V_f^h}\right\} \\ &= \widehat{\omega}_f + \Re\left\{\frac{1}{2i\pi}\frac{V_f^hV_f^{th}}{V_f^hV_f^{t^2h} - (V_f^{th})^2}\right\} - \Im\left\{\frac{1}{\sigma^2}\frac{V_f^{th}}{V_f^h}\right\} \\ &= \widehat{\omega}_f + \Re\left\{\frac{1}{2i\pi}\frac{V_f^hV_f^{th}}{V_f^hV_f^{t^2h} - (V_f^{th})^2}\right\} - (\widehat{\omega}_f - \eta) \\ &= \eta + \Im\left\{\frac{1}{2\pi}\frac{V_f^hV_f^{th}}{V_f^hV_f^{t^2h} - (V_f^{th})^2}\right\}. \end{aligned} \tag{20}$$

An alternative technique to compute and LIF estimator still assuming a local linear chirp approximation for the modes is to consider that the complex modulation operator is not defined by (7) but obtained as follows [19]:

$$\bar{q}_f = \frac{\partial_t\tilde{\omega}_f}{\partial_t\tilde{t}_f} = \frac{1}{2i\pi}\frac{V_f^{h''}V_f^h - (V_f^{h'})^2}{V_f^{th}V_f^{h'} - V_f^{th'}V_f^h}. \tag{21}$$

Replacing $\tilde{q}_f$ by $\bar{q}_f$ in (8), one obtains a new LIF estimator, which is actually the same as the one introduced in [21]. Indeed, one has

$$\begin{aligned} &\frac{1}{2i\pi}\frac{V_f^{h''}V_f^h - (V_f^{h'})^2}{V_f^{th}V_f^{h'} - V_f^{th'}V_f^h} \\ = &\frac{1}{2i\pi}\frac{(-V_f^h + \frac{2\pi}{\sigma^2}V_f^{t^2h})V_f^h - \frac{2\pi}{\sigma^2}(V_f^{th})^2}{-(V_f^{th})^2 + V_f^{t^2h}V_f^h} \\ = &\frac{1}{i\sigma^2} - \frac{(V_f^h)^2}{2i\pi(V_f^{t^2h}V_f^h - (V_f^{th})^2)}, \end{aligned} \tag{22}$$

and the LIF estimator obtained using $\bar{q}_f$ instead of $\tilde{q}_f$ reads:

$$\begin{aligned} \bar{\omega}_f^{[2]} &= \widehat{\omega}_f + \Re\left\{(-\frac{1}{i\sigma^2} + \frac{(V_f^h)^2}{2i\pi(V_f^{t^2h}V_f^h - (V_f^{th})^2)})\frac{V_f^{th}}{V_f^h}\right\} \\ &= \widehat{\omega}_f + \Re\left\{\frac{V_f^hV_f^{th}}{2i\pi(V_f^{t^2h}V_f^h - (V_f^{th})^2)}\right\} - \Im\left\{\frac{1}{\sigma^2}\frac{V_f^{th}}{V_f^h}\right\} \\ &= \widehat{\omega}_f^{[2]}. \end{aligned} \tag{23}$$

As far as higher order LIF estimators, i.e. $N > 2$, are concerned, to use the Gaussian window also brings interesting simplifications. Indeed, in such a case the first two columns of matrix V_1 introduced in (17) are colinear and thus its determinant of is null. In that context, we may thus write:

$$\widehat{\omega}_f^{[N]} = \frac{1}{2\pi}\Im\left\{r_1^{[N]}\right\} = \eta - \frac{1}{2\pi}\Im\left\{\frac{det(U_1)}{det(D)}\right\}. \tag{24}$$

In the following sections, we will stick to the use of the Gaussian window since the studied LIF estimators have simpler forms.

III. On Approximations of Reassignment Vectors in the Vicinity of their Zeros

In this section, we first investigate more in details the nature of the zeros of the reassignment vectors namely of $\widehat{\omega}_f^{[N]}(t,\eta) - \eta$, focusing in particular on the cases $N = 1$ and $N = 2$. Then we propose different simple approximations of reassignment vectors in the vicinity of their zeros that will help us understand the differences between reassignment processes.

A. Characterization of the Zeros of Reassignment Vectors

To study the zeros of the reassignment vector, when $N = 1$, we first recall that (omitting again (t,η) for the sake of simplicity):

$$\begin{aligned} \widehat{\omega}_f - \eta &= \Im\left\{\frac{1}{\sigma^2}\frac{V_f^{th}}{V_f^h}\right\} \\ &= -\Im\left\{\frac{1}{2i\pi\sigma^2}\frac{\partial_\eta V_f^h}{V_f^h}\right\} = \frac{1}{4\pi\sigma^2}\frac{\partial_\eta|V_f^h|^2}{|V_f^h|^2}, \end{aligned} \tag{25}$$

whose zeros correspond to the points (t,η) such that $\partial_\eta|V_f^h(t,\eta)|^2 = 0$.

Now, we investigate the zeros of $\widehat{\omega}_f^{[2]}(t,\eta)-\eta$ corresponding to:

$$\widehat{\omega}_f^{[2]}(t,\eta)-\eta = \Im\left\{\frac{1}{2\pi}\frac{V_f^h V_f^{th}}{V_f^h V_f^{t^2h}-(V_f^{th})^2}\right\}=0 \quad (26)$$

that is to say

$$\begin{aligned}&\Im\left\{V_f^h V_f^{th}(V_f^h V_f^{t^2h}-(V_f^{th})^2)^*\right\}=0\\ \Leftrightarrow\ &|V_f^h|^2\Im\left\{V_f^{th}(V_f^{t^2h})^*\right\}-|V_f^{th}|^2\Im\left\{V_f^h(V_f^{th})^*\right\}=0\\ \Leftrightarrow\ &|V_f^h|^2\Re\left\{V_f^{th}\partial_\eta(V_f^{th})^*\right\}-|V_f^{th}|^2\Re\left\{V_f^h\partial_\eta(V_f^h)^*\right\}=0\\ \Leftrightarrow\ &|V_f^h|^2\partial_\eta|V_f^{th}|^2-|V_f^{th}|^2\partial_\eta|V_f^h|^2=0.\end{aligned} \quad (27)$$

which can also be viewed as

$$det\begin{bmatrix}|V_f^h|^2 & \partial_\eta|V_f^h|^2\\ |V_f^{th}|^2 & \partial_\eta|V_f^{th}|^2\end{bmatrix}=0.$$

The reassignment vector when $N=2$ thus reads:

$$\widehat{\omega}_f^{[2]}-\eta=\frac{|V_f^h|^2\partial_\eta|V_f^{th}|^2-|V_f^{th}|^2\partial_\eta|V_f^h|^2}{|V_f^h V_f^{t^2h}-(V_f^{th})^2|^2}, \quad (28)$$

and the zeros of this reassignment vector are attractive or repulsive points, when the derivative of $|V_f^h|^2\partial_\eta|V_f^{th}|^2-|V_f^{th}|^2\partial_\eta|V_f^h|^2$ is non zero at these locations.

To extend (27) to higher order N could be carried out by considering the points (t,η) such that $\Im\{det(U_1)det(D)^*\}=0$, but this leads to much more complex expressions, whose analysis is left for future work.

B. Approximating Reassignment Vectors in the Vicinity of their Zeros

We are now interested in approximating the different reassignment vectors in the vicinity of their zeros. We first approximate second order reassignment vector, i.e. $N=2$, considering that, in the vicinity of its zeros, V_f^{th} is small, bearing in mind that for a linear chirp it is proven to be equal to 0 at these zeros. We thus consider the following approximation of $\widehat{\omega}_f^{[2]}(t,\eta)$ in the vicinity of its fixed points (i.e. the zeros of $\widehat{\omega}_f^{[2]}(t,\eta)-\eta$):

$$\begin{aligned}\widehat{\omega}_f^{[2]}(t,\eta)&=\eta+\Im\left\{\frac{1}{2\pi}\frac{V_f^h V_f^{th}}{V_f^h V_f^{t^2h}-(V_f^{th})^2}\right\}\\ &=\eta+\Im\left\{\frac{1}{2\pi}\frac{V_f^{th}}{V_f^{t^2h}}\frac{1}{1-\frac{(V_f^{th})^2}{V_f^h V_f^{t^2h}}}\right\}\\ &\approx\eta+\Im\left\{\frac{1}{2\pi}\frac{V_f^{th}}{V_f^{t^2h}}\right\}+\Im\left\{\frac{1}{2\pi}\frac{(V_f^{th})^3}{V_f^h(V_f^{t^2h})^2}\right\}.\end{aligned} \quad (29)$$

When $\frac{(V_f^{th})^2}{V_f^h V_f^{t^2h}}<<1$, one can approximate $\widehat{\omega}_f^{[2]}$ only including the first order term in V_f^{th} in approximation (29), which we denote by $\widehat{\omega}_{f,1}^{[2]}$. In the opposite case, one should consider two terms in the approximation, namely third order terms in V_f^{th}. We denote by $\widehat{\omega}_{f,2}^{[2]}$ this approximation.

From now on, we call *second order zeros* the zeros of $\widehat{\omega}_f^{[2]}(t,\eta)-\eta$, and we now define approximations of $\widehat{\omega}_f^{[3]}$ in the vicinity of these points when f is a monocomponent satisfying (9) with A constant. For that purpose, we first rewrite $\widehat{\omega}_f^{[3]}(t,\eta)$ as a perturbation of $\widehat{\omega}_f^{[2]}(t,\eta)$, and show the following relation between second and third order reassignment operators:

Proposition III.1. *Assume f satisfies* (9) *with A constant, then we have:*

$$\widehat{\omega}_f^{[3]}=\widehat{\omega}_f^{[2]}+\Im\left\{\frac{r_3^{[3]}}{2\pi}\right\}\Re\left\{\frac{(V_f^{t^2h})^2-V_f^{t^3h}V_f^{th}}{(V_f^{th})^2-V_f^{t^2h}V_f^h}\right\} \quad (30)$$

The proof is available in Appendix A.

From this, we deduce that at a zero (t,η_0) of $\widehat{\omega}_f^{[2]}(t,\eta)-\eta$ one has:

$$\begin{aligned}&\widehat{\omega}_f^{[3]}(t,\eta_0)\\ &\approx\eta_0+\Im\left\{\frac{r_3^{[3]}(t,\eta_0)}{2\pi}\right\}\Re\left\{\frac{(V_f^{t^2h})^2-V_f^{t^3h}V_f^{th}}{(V_f^{th})^2-V_f^{t^2h}V_f^h}\right\}\end{aligned} \quad (31)$$

Assuming that both V_f^{th} and $V_f^{t^3h}$ are small at this point, we get the following approximation of $\widehat{\omega}_f^{[3]}$:

$$\widehat{\omega}_{f,1}^{[3]}(t,\eta_0) = \eta_0+\Im\left\{\frac{r_3^{[3]}(t,\eta_0)}{2\pi}\right\}\Re\left\{\frac{-V_f^{t^2h}}{V_f^h}\right\}.$$

To investigate the role played by the term $V_f^{t^3h}$, we also consider the following approximation of $\widehat{\omega}_f^{[3]}$ in which we only neglect the second order terms in V_f^{th}:

$$\begin{aligned}&\widehat{\omega}_{f,2}^{[3]}(t,\eta_0)=\\ &\eta_0+\Im\left\{\frac{r_3^{[3]}(t,\eta_0)}{2\pi}\right\}\Re\left\{\frac{-V_f^{t^2h}}{V_f^h}+\frac{V_f^{t^3h}V_f^{th}}{V_f^{t^2h}V_f^h}\right\}.\end{aligned} \quad (32)$$

We will investigate this different types of approximation later in numerical applications.

IV. Analysis of Reassignment Vectors on Interfering Pure Harmonic Modes

In this section we study the behavior of reassignment vectors when the signal is made of interfering pure harmonics. First, we investigate the zeros of the reassignment vectors when $N=1$ or $N=2$, and the behavior of the latter in the vicinity of *spectrogram ridges*, corresponding to the points $\partial_\eta|V_f^h(t,\eta)|^2=0$. We then propose a new technique to retrieve the IFs of the modes making up the signal by studying the reassigned transforms. Finally, we investigate the behavior of the third order reassignment vector in that context.

Let us consider that $f(t)=f_1(t)+f_2(t)$ with $f_1(t)=Ae^{i2\pi\xi_1 t}$ and $f_2(t)=e^{i2\pi\xi_2 t}$, where $\xi_1<\xi_2$. For such a signal and when h is the Gaussian window mentioned above, one has $V_{f_1}^h(t,\eta)=\hat{h}(\eta-\xi_1)Ae^{i2\pi\xi_1 t}=\sigma Ae^{i2\pi\xi_1 t}e^{-\pi(\eta-\xi_1)^2\sigma^2}$ and $V_{f_2}^h(t,\eta)=\sigma e^{i2\pi\xi_2 t}e^{-\pi(\eta-\xi_2)^2\sigma^2}$, and the spectrogram reads:

$$\begin{aligned}|V_f^h(t,\eta)|^2=\sigma^2(&A^2e^{-2\pi\sigma^2(\eta-\xi_1)^2}+e^{-2\pi\sigma^2(\eta-\xi_2)^2}\\ &+2Ae^{-\pi\sigma^2\left[(\eta-\xi_1)^2+(\eta-\xi_2)^2\right]}\cos(2\pi(\xi_2-\xi_1)t))\end{aligned} \quad (33)$$

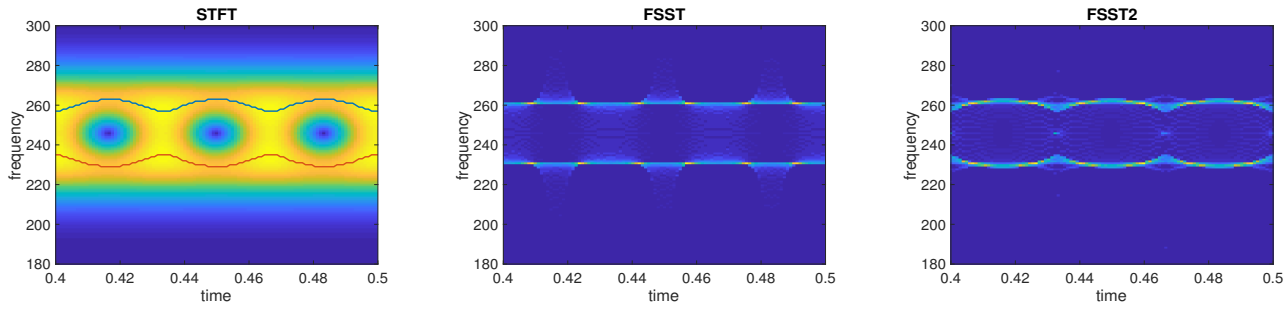

(a) (b) (c)

Fig. 1: (a): STFT of two interfering modes, with the two ridges associated with local maxima superimposed; (b): FSST of the signal in (a); (c): FSST2 of the signal in (a)

A. Determination of the Zeros Common to First and Second Order Reassignment Vectors

We here investigate the set of TF points consisting of the zeros common to the first and second order reassignment vector. In the previous, section we showed that the zeros at time t of $\widehat{\omega}_f - \eta$ corresponded to η satisfying $\partial_\eta |V_f^h(t,\eta)|^2 = 0$ and $V_f^h(t,\eta) \neq 0$. We can then prove the following result:

Proposition IV.1. *A zero (t,η) of $\widehat{\omega}_f - \eta$, such that $V_f^h V_f^{t^2 h} - (V_f^{th})^2 \neq 0$ is a zero of $\widehat{\omega}_f^{[2]} - \eta$ if and only if*

$$A(\eta-\xi_1)e^{-\pi\sigma^2(\eta-\xi_1)^2} = \pm(\eta-\xi_2)e^{-\pi\sigma^2(\eta-\xi_1)^2}$$

The proof is available in Appendix B. The time instants associated with these points then obey the following rule:

Proposition IV.2. *If (t,η) is a zero common to $\widehat{\omega}_f - \eta$ and $\widehat{\omega}_f^{[2]} - \eta$ such that $A(\eta-\xi_1)e^{-\pi\sigma^2(\eta-\xi_1)^2} = -(\eta-\xi_2)e^{-\pi\sigma^2(\eta-\xi_1)^2}$ (resp. $A(\eta-\xi_1)e^{-\pi\sigma^2(\eta-\xi_1)^2} = (\eta-\xi_2)e^{-\pi\sigma^2(\eta-\xi_1)^2}$), then $t = t_k = \frac{k}{\xi_2-\xi_1}$ for some $k \in \mathbb{Z}$ (resp. $\tilde{t}_k = \frac{k+1/2}{\xi_2-\xi_1}$ for some $k \in \mathbb{Z}$).*

The proof is available in Appendix C. Note that the time instants t_k when k varies (resp. $\tilde{t}_k$) are associated with local maxima (resp. minima) of $|V_f^h(.,\eta)|^2$. Furthermore, we can also remark that the locations t_k (resp. $\tilde{t}_k$) correspond to local maxima (resp. minima) of the spectrogram along the spectrogram ridges.

B. Analysis of Second Order Reassignment Vector in the Vicinity of Spectrogram Ridges

Let us first remark that at location t_k and $\tilde{t}_k$ defined in the previous section we have for any η:

$$\begin{aligned} |V_f^h(t_k,\eta)|^2 &= (Ae^{-\pi\sigma^2(\eta-\xi_1)^2} + e^{-\pi\sigma^2(\eta-\xi_2)^2})^2 \\ |V_f^h(\tilde{t}_k,\eta)|^2 &= (Ae^{-\pi\sigma^2(\eta-\xi_1)^2} - e^{-\pi\sigma^2(\eta-\xi_2)^2})^2 \end{aligned} \quad (34)$$

At time t_k, when the level of interference is not too high $|V_f^h(t_k,.)|^2$ has three extrema, located respectively at $\eta_0^{\max} < \eta_1^{\max} < \eta_2^{\max}$. We use the superscript max to recall that $|V_f^h(.,\eta)|^2$ is maximum at t_k. Note that $\eta_0^{\max}$ and $\eta_2^{\max}$ correspond to maxima and $\eta_1^{\max}$ to a minimum of $|V_f^h(t_k,.)|^2$. Similarly, at time $\tilde{t}_k$, $|V_f^h(\tilde{t}_k,.)|^2$ has three extrema located at $\eta_0^{\min} < \eta_1^{\min} < \eta_2^{\min}$ (the superscript min recalling that $|V_f^h(.,\eta)|^2$ is minimum at $\tilde{t}_k$). Note that $\eta_0^{\min}$ and $\eta_2^{\min}$ correspond to maxima and $\eta_1^{\min}$ to a minimum of $|V_f^h(\tilde{t}_k,.)|^2$. Finally, one can also remark that the point $(\tilde{t}_k, \eta_1^{\min})$ is a zero of the spectogram.

The points $(t_k, \eta_2^{\max})$ and $(\tilde{t}_k, \eta_2^{\min})$ are part of what we call from now on the upper spectrogram ridge (see the blue curve in Fig. 1 (a)) , while $(t_k, \eta_0^{\max})$ and $(\tilde{t}_k, \eta_0^{\min})$ belong to the lower spectrogram ridge (see the red curve in Fig. 1 (a)). Investigating the behavior of the second order reassignment vector on the upper and lower spectrogram ridges, we find the following property:

Proposition IV.3. *On the upper (resp. lower) spectrogram ridge the second order reassignment vector is oriented towards higher (resp. lower) frequencies except at points corresponding to time instants t_k and $\tilde{t}_k$.*

The proof is available in Appendix D. An illustration of Proposition IV.3 is given in Fig. 1 (c), in which we see, by comparing with Fig. 1 (a), that the TF coefficients are not reassigned onto the spectrogram ridges with FSST2: the point on the upper (resp. lower) spectrogram ridge (except those at time t_k and $\tilde{t}_k$) are reassigned at a higher frequency (resp. lower) frequency. Finally, note that, even if the spectrogram ridges are the zeros of the first order reassignment vector, this does mean *FSST ridges*, i.e. TF curves corresponding to local maxima of the modulus of FSST along the frequency axis, are the same as the spectrogram ridges (see Fig. 1 (b)).

C. New IF Estimator from the Ridges of the Reassigned Transforms

From Fig. 1, it transpires that neither the spectrogram ridges nor *FSST2 ridges*, i.e. TF curves corresponding to local maxima of the modulus of FSST2 along the frequency axis, are good estimates of the IF of the modes.

We are now going to explain how to use the ridges of the reassigned transforms to define a new technique for the estimation of the IFs of the modes. For that purpose, we shall first remark that at points $\bar{t}_k = \frac{2k+1}{4(\xi_2-\xi_1)}$, the spectrogram reads

$$\begin{aligned} |V_f^h(\bar{t}_k,\eta)|^2 &= \sigma^2(A^2 e^{-2\pi\sigma^2(\eta-\xi_1)^2} + e^{-2\pi\sigma^2(\eta-\xi_2)^2}) \\ &= |V_{f_1}^h(\bar{t}_k,\eta)|^2 + |V_{f_2}^h(\bar{t}_k,\eta)|^2. \end{aligned} \quad (35)$$

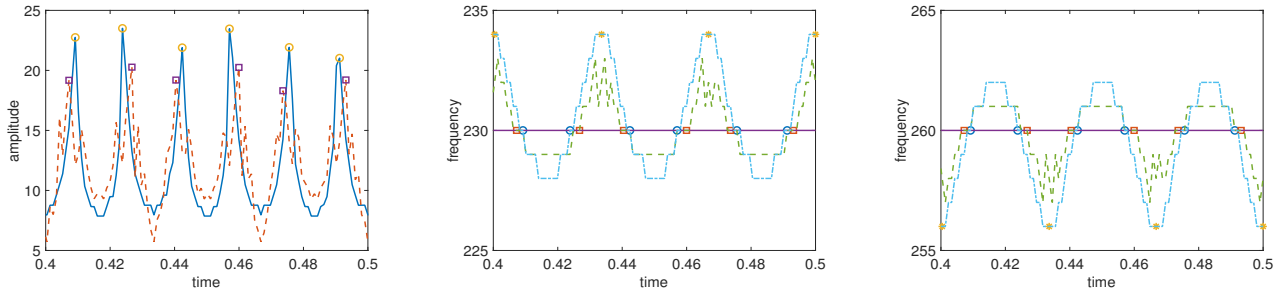

(a) (b) (c)

Fig. 2: (a): moduli of FSST and FSST2 along their upper ridge for the FSST of Fig. 1 (b) and (c) (plain line corresponds to FSST and dashed line to FSST2, circles and squares are located at the local maxima in each case); (b): lower ridges for STFT (dashed dotted line), FSST (plain line) and FSST2 (dashed line) (the stars, circles and squares denote the locations of the local maxima of the modulus of each TFR along the corresponding ridge); (c): same as (b) but for the upper ridge.

This means that, at these points, STFT does not see mode interference, therefore the points on the spectrogram ridge at these time instants should give the best estimate of the IFs of the modes. However, to determine the time instants $\bar{t}_k$ is not possible because it explicitly uses ξ_1 and ξ_2 the unknown frequencies.

Note that FSST should be sharp at these points because the corresponding reassignment vector is only slightly contaminated by mode interference. Based on this remark, we propose a novel strategy to estimate the IF of the modes by considering the most significant maxima of the modulus of FSST along its ridges, and then by defining an IF estimator as the frequency locations of these maxima. An estimator of $\bar{t}_k$ can also be obtained by considering the time instants of these maxima.

Interestingly, these time instants $\bar{t}_k$ are also critical for the second order reassignment operator. Indeed, recalling that we have:

$$V_f^{th} = \frac{1}{2i\pi}\partial_\eta V_f^h = \frac{\sigma^3}{i}\Big[A(\eta-\xi_1)e^{-\pi\sigma^2(\eta-\xi_1)^2}e^{2i\pi\xi_1 t} + (\eta-\xi_2)e^{-\pi\sigma^2(\eta-\xi_2)^2}e^{2i\pi\xi_2 t}\Big] \quad (36)$$

one obtains that, at $t=\bar{t}_k$:

$$|V_f^{th}(\bar{t}_k,\eta)|^2 = |V_{f_1}^{th}(\bar{t}_k,\eta)|^2 + |V_{f_2}^{th}(\bar{t}_k,\eta)|^2. \quad (37)$$

Then the numerator of (28) is made of expressions that clearly separate the first mode from the second, and thus FSST2 should also be sharp at $\bar{t}_k$. A new IF estimator can then be obtained by considering again the most significant maxima of FSST2 modulus along FSST2 ridges, and then the points $\bar{t}_k$ could be estimated as the time locations of these maxima.

To illustrate the new strategy for IF estimation, we plot in Fig. 2 (a), the modulus of FSST and FSST2 along their upper ridges, and notice that their most significant local maxima are very close in time, which is in accordance with the fact their time locations are estimates of time instants $\bar{t}_k$. To check the relevance of these time indices for IF estimation, we plot in Fig. 2 (b) and (c), STFT, FSST and FSST2 lower and upper ridges respectively as well as the locations of the local maxima of their moduli. We notice that the locations of the local maxima of the moduli of FSST and FSST2 actually correspond to the IF of each mode and that the locations of these maxima are close to the time locations where the spectrogram ridges pass through the true IF. We also remark that the ridges associated with FSST are at the expected IF location, while the ridges of FSST2 are closer to those of the spectrogram (though higher (resp. lower) for the upper (resp. lower) ridge than the upper (resp. lower) spectrogram ridge as predicted by Proposition IV.3).

To explain why FSST ridges consist of a better IF estimator than FSST2 ridges, we plot $\widehat{\omega}_f$ and $\widehat{\omega}_f^{[2]}$ in the vicinity of the lower spectrogram ridge, at location t_k and $\tilde{t}_k$, in Fig. 3 (a) and (b). We notice, at location t_k, that, as one moves away from the spectrogram ridge towards lower frequency, $\widehat{\omega}_f$ is much more accurate than $\widehat{\omega}_f^{[2]}$. From Fig. 3 (b), a similar conclusion can be drawn at time $\tilde{t}_k$. This explains why FSST ridge is a better IF estimator than FSST2 ridge. To better understand the behavior of $\widehat{\omega}_f^{[2]}$ in the vicinity of the lower spectrogram ridge, we also plot in Fig. 3 (c) and (d) its approximations $\widehat{\omega}_{f,1}^{[2]}$ and $\widehat{\omega}_{f,2}^{[2]}$, defined right after (29), at time t_k and $\tilde{t}_k$. While close to the ridge these approximations are correct, the hypothesis that V_f^{th} is small becomes rapidly erroneous as one moves away from the spectrogram ridge towards lower frequencies, and the proposed simple approximation of $\widehat{\omega}_f^{[2]}$ are no longer valid.

D. Behavior of Third Order Synchrosqueezing Transform in the Vicinity of Spectogram Ridges

Let us consider the point on the lower spectrogram ridge at time $\tilde{t}_k$, which is a zero of $\widehat{\omega}_f^{[2]}-\eta$. Denote by $(t,\psi_0'(t))$ the spectrogram ridge in the vicinity of that point. We first remark that $\Im\left\{\frac{r_3^{[3]}(t,\psi_0'(t))}{2\pi}\right\} \approx \psi_0^{(3)}(t)$ which is such that $\psi_0^{(3)}(\tilde{t}_k)>0$ (see Fig. 1 (a), lower ridge). Then making a pure harmonic approximation, we get that $\Re\left\{\frac{-V_f^{t^2h}}{V_f^h}\right\} \approx -\sigma^2 < 0$ at these points. From this, we deduce that the zeros of $\widehat{\omega}_f^{[2]}-\eta$ are reassigned towards lower frequency using $\widehat{\omega}_{f,1}^{[3]}$. As $\widehat{\omega}_{f,1}^{[3]}$

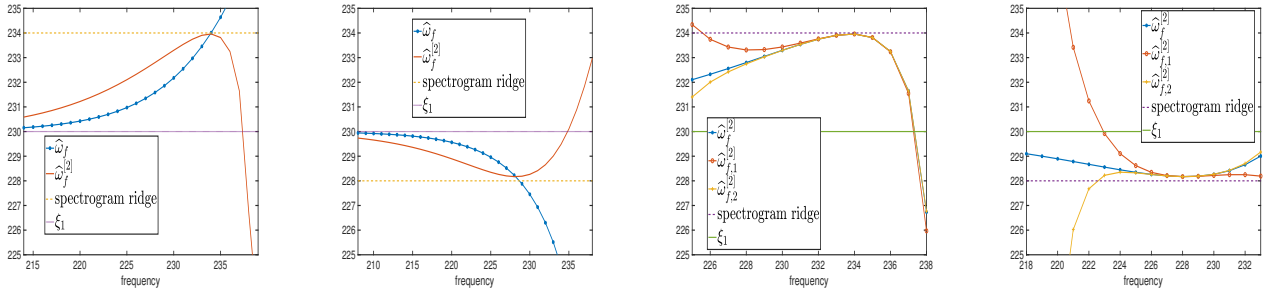

(a) (b) (c) (d)

Fig. 3: (a): $\widehat{\omega}_f$ and $\widehat{\omega}_f^{[2]}$ in the vicinity of the lower spectrogram ridge at time t_k; (b): same as (a) but at time $\tilde{t}_k$; (c): $\widehat{\omega}_f^{[2]}$, $\widehat{\omega}_{f,1}^{[2]}$, and $\widehat{\omega}_{f,2}^{[2]}$ in the vicinity of the lower spectrogram ridge at time t_k; (d): same as (c) but at time $\tilde{t}_k$.

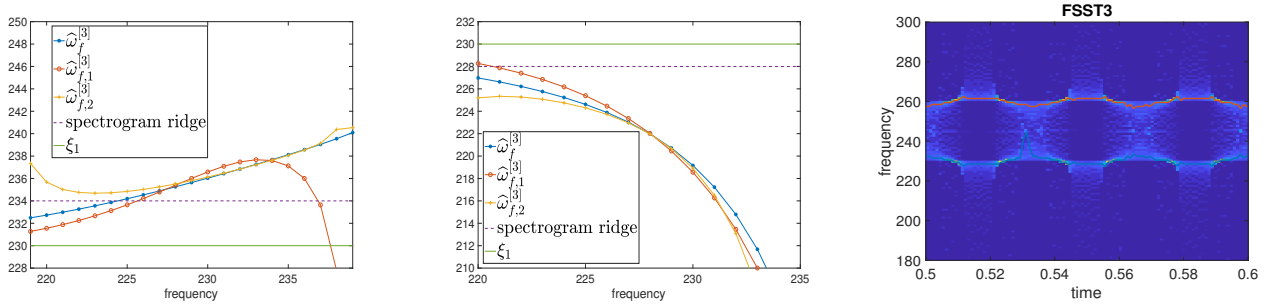

(a) (b) (c)

Fig. 4: (a): $\widehat{\omega}_f$, $\widehat{\omega}_f^{[2]}$, $\widehat{\omega}_f^{[3]}$ and its approximation around TF point $(t_k, \eta_1^{\max})$; (b): same as (a) but around point $(\tilde{t}_k, \eta_1^{\min})$; (c): modulus of FSST3 for the interfering modes along with the corresponding ridges.

is a good approximation of $\widehat{\omega}_f^{[3]}$ at that point (see Fig. 4 (b)), such will also be the case when one uses $\widehat{\omega}_f^{[3]}$: the reassigned value when using $\widehat{\omega}_f^{[3]}$ are farther from ξ_1 than the one given $\widehat{\omega}_f$ or $\widehat{\omega}_f^{[2]}$. Similarly, at time t_k, still on the lower spectrogram ridge, the third order reassignment vector is oriented upward (see Fig. 4 (a)), since $\psi_0^{(3)}(t_k) < 0$ and using the same pure harmonic approximation as previously (remarking $\widehat{\omega}_{f,1}^{[3]}$ is still a good approximation of $\widehat{\omega}_f^{[3]}$ (see Fig. 4 (c))). The reassigned value is again farther from ξ_1 than the one given $\widehat{\omega}_f$ or $\widehat{\omega}_f^{[2]}$. The modulus of FSST3 for the signal of Fig. 1 (a) along with its ridges are finally displayed in Fig. 4 (c), and we notice that ridge detection is less accurate in that case.

V. Analysis of Reassignment Vectors on Noisy Monocomponent Signals

In this section, we first investigate the nature of the zeros common to first and second order reassignment vectors in the case of a linear chirp, then we study the behavior of reassignment vectors on different noisy signals and propose a new technique for IF estimation based on significant local maxima along the ridges of the reassigned transforms. Finally, we explain why in such a context IF estimators based on higher order reassignment operators should be precluded.

A. Determination of the Common Zeros of First and Second Reassignment Vectors

Let us first remark that the STFT of a linear chirp $f(t) = Ae^{2i\pi\phi(t)}$ computed with the Gaussian window $g(t) = e^{-\pi\frac{t^2}{\sigma^2}}$ reads [19]:

$$V_f^h(t,\eta) = V_f^h(t,\phi'(t))e^{\frac{-\pi\sigma^2(1+i\phi''(t)\sigma^2)}{1+(\phi''(t)\sigma^2)^2}(\eta-\phi'(t))^2}. \quad (38)$$

From this we immediately get that:

$$\begin{aligned} V_f^{t^k h}(t,\eta) &= \left(\frac{i}{2\pi}\right)^k \partial_\eta^k V_f^h(t,\eta) = \\ &\left(\frac{i}{2\pi}\right)^k \partial_\eta^{k-1}\left[\frac{-2\pi\sigma^2(1+i\phi''(t)\sigma^2)}{1+(\phi''(t)\sigma^2)^2}(\eta-\phi'(t))V_f^h(t,\eta)\right] \\ &= \left(\frac{i}{2\pi}\right)^k \frac{-2\pi\sigma^2(1+i\phi''(t)\sigma^2)}{1+(b\sigma^2)^2} \quad (39) \\ &\left[(\eta-\phi'(t))\partial_\eta^{k-1}V_f^h(t,\eta) + (k-1)\partial_\eta^{k-2}V_f^h(t,\eta)\right] \\ &= \frac{-2\pi\sigma^2(1+i\phi''(t)\sigma^2)}{1+(\phi''(t)\sigma^2)^2} \\ &\left[(\eta-\phi'(t))\frac{i}{2\pi}V_f^{t^{k-1}h}(t,\eta) - (k-1)\frac{1}{4\pi^2}V_f^{t^{k-2}h}(t,\eta)\right]. \end{aligned}$$

Thus, $V_f^{t^k h}(t,\phi'(t))$ is null when k is odd, which enables us to deduce the following proposition.

Proposition V.1. *The zeros of $\widehat{\omega}_f - \eta$ and $\widehat{\omega}_f^{[2]} - \eta$ are the*

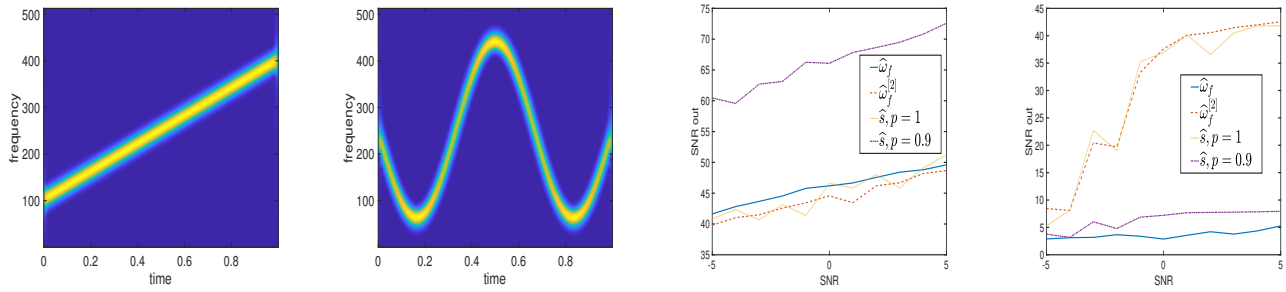

(a) (b) (c) (d)

Fig. 5: (a):Modulus of the STFT of a linear chirp; (b): Modulus of the STFT of a signal with cosinusoidal phase; (c): output SNR associated with IF estimation $\widehat{s}$, $\widehat{\omega}$ and $\widehat{\omega}^{[2]}$ for noisy version of signal (a), with respect to input SNR (the results are averaged over 20 noise realizations); (d): same as (c) but for the signal displayed in (b).

same.

Proof: Indeed assume, (t,η) is a zero of $\widehat{\omega}_f - \eta$, that is we have $\partial_\eta |V_f^h(t,\eta)|^2 = 0$ which is equivalent to $\eta = \phi'(t)$. Now let us compute

$$\begin{aligned} &\partial_\eta |V_f^{th}(t,\eta)|^2 \\ &= \frac{\sigma^4}{1+(\phi''(t)\sigma^2)^2} \partial_\eta \left[(\eta - \phi'(t))^2 |V_f^h(t,\eta)|^2 \right] \\ &= \frac{\sigma^4}{1+(\phi''(t)\sigma^2)^2} \\ &\left[2(\eta - \phi'(t)) |V_f^h(t,\eta)|^2 + (\eta - \phi'(t))^2 \partial_\eta |V_f^h(t,\eta)|^2 \right], \end{aligned} \tag{40}$$

from which we get that

$$\begin{aligned} &|V_f^h(t,\eta)|^2 \partial_\eta |V_f^{th}(t,\eta)|^2 - |V_f^{th}(t,\eta)|^2 \partial_\eta |V_f^h(t,\eta)|^2 \\ &= \frac{\sigma^4 2(\eta - \phi'(t))}{1+(\phi''(t)\sigma^2)^2} |V_f^h(t,\eta)|^4 \end{aligned} \tag{41}$$

which is null if and only if $\eta = \phi'(t)$, meaning the zeros of the first and second order reassignment operators are the same. ■

B. New IF Estimator from the Ridges of the Reassigned Transforms

We here consider some complex Gaussian white noise n is added to the monocomponent signal f to obtain $\tilde{f} = f + n$, the zeros of $\widehat{\omega}_{f+n} - \eta$ still correspond to the points (t,η) satisfying $\partial_\eta |V_{f+n}^h(t,\eta)|^2 = 0$. So, if f is a linear chirp, the zeros of the first order reassignment vector are no longer located at $\eta = \phi'(t)$ and the noise also creates new zeros for that reassignment vector that are not related to the signal. In that context, the zeros of $\widehat{\omega}_{f+n} - \eta$ are different but close to those of $\widehat{\omega}_{f+n}^{[2]} - \eta$.

Another important aspect is that the presence of noise creates some oscillations of the amplitude of the modulus of the STFT along spectrogram ridges. As in the case of interfering mode, we hypothesize that the most significant FSST2 modulus maxima along these ridges are also those the least impacted by noise. In this regard, note that most ridge detectors adopt a very similar point of view by considering that the largest modulus maxima of STFT are most probably related to the signal [8], [30], [31]. So, we propose to compute a new IF estimator using a cubic spline approximation of the most significant modulus maxima along FSST2 ridge. Namely, if we denote by $\mathcal{M}$ this set we consider the cubic spline:

$$\widehat{s} = \underset{s \in \mathcal{S}}{\operatorname{argmin}} \left[p \sum_{[n,k] \in \mathcal{M}} |k - s(\frac{n}{L})|^2 + (1-p) \int |s^{(2)}(t)| dt \right], \tag{42}$$

where $\mathcal{S}$ is the set of cubic spline, and p is trade-off parameter between the data term and the smoothing term. We display in Fig. 5 (c) and (d), the output SNR associated with IF estimator $\widehat{s}$, for different values of p, along with $\widehat{\omega}$ and $\widehat{\omega}^{[2]}$ for the two signals of Fig. 5 (a) and (b), and when the input SNR varies. In the case of a linear chirp, corresponding to the results of Fig. 5 (c), the IF estimators based on $\widehat{s}$, with no smoothing, $\widehat{\omega}$ and $\widehat{\omega}^{[2]}$ are very similar, meaning the information contained in the significant modulus maxima along the FSST2 ridge is sufficient to obtained a performant IF estimator. Then, as by putting $p = 0.9$ one obtains a significantly better IF estimator, in the case of a linear chirp, smoothing is essential to improve IF estimation. Considering the signal with cosinusoidal phase of Fig. 5 (b), we get that IF estimator $\widehat{s}$ without smoothing behaves similarly to $\widehat{\omega}^{[2]}$, meaning again that the significant modulus maxima along the FSST2 ridge contain enough information to perform IF estimation. Note finally that in such a case no smoothing should be used and that IF estimator degrades significantly at negative input SNR mainly because ridge detection fails in some instances.

C. Behavior of Higher Order Reassignment Operator on Noisy Linear Chirps

As in the case of two pure harmonics interfering, we here analyze the behavior of $\widehat{\omega}_{f+n}^{[3]}$ in the vicinity of the zeros of $\widehat{\omega}_{f+n}^{[2]} - \eta$. At these points, which are located on some ridge $(t, \psi'(t))$, we still have:

$$\begin{aligned} &\widehat{\omega}_{f+n}^{[3]}(t,\psi'(t)) - \eta \approx \\ &\Im \left\{ \frac{r_3^{[3]}(t,\psi'(t))}{2\pi} \right\} \Re \left\{ \frac{(V_{f+n}^{t^2h})^2 - V_{f+n}^{t^3h} V_{f+n}^{th}}{(V_{f+n}^{th})^2 - V_{f+n}^{t^2h} V_{f+n}^{h}} \right\} \end{aligned} \tag{43}$$

Following what was done in the case of interference we numerically notice that $\Re\left\{\frac{(V_{f+n}^{t^2h})^2-V_{f+n}^{t^3h}V_{f+n}^{th}}{(V_{f+n}^{th})^2-V_{f+n}^{t^2h}V_{f+n}^{h}}\right\}$ remains negative on $(t,\psi'(t))$ thus $\widehat{\omega}_{f+n}^{[3]}(t,\psi'(t))-\eta$ is positive when $\psi'(t)$ is concave and negative otherwise. The consequence of this is that if the ridge $(t,\psi'(t))$ is oscillating then FSST3 ridge oscillates even more. To confirm this, we consider a noisy linear chirp

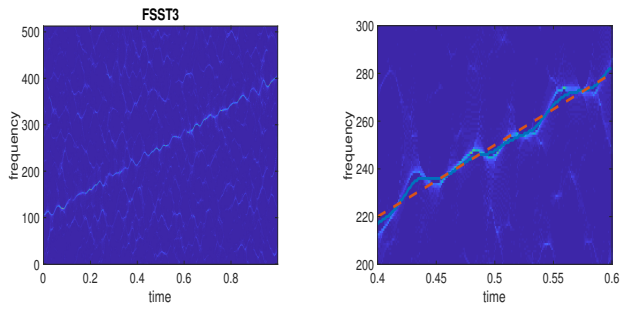

(a) (b)

Fig. 6: (a): Modulus of FSST3 for a noisy linear chirp (SNR equal -5 dB); (b): zoom in on FSST3 modulus, on which FSST2 ridge (plain line) and the true IF (dashed line) are superimposed

whose FSST3 modulus is displayed in Fig. 6 (a), and a zoomed in version in Fig. 6 (b), on which we superimpose FSST2 ridge (plain line) and true IF (dashed line). We notice that, as expected, when the FSST2 ridge oscillates, FFST3 ridge oscillates even more: this is accordance with the study of the third order reassignment vector depending on the concavity of $\psi'(t)$, and thus IF estimation from FSST3 ridge is less accurate than that based FSST2 ridge on that type of noisy signals.

VI. Conclusion

In this paper, we proposed to analyze the behavior of the reassignment vectors used in synchrosqueezing transforms in various situations. Our goal was first to investigate more in details the zeros of reassignment vectors, and then to study reassignment vectors applied to interfering pure harmonic modes and then to noisy mono-component signal. From our study, it transpired that the TF coefficients are reassigned to very different locations depending on the order of the reassignment vector, and the ridges of the reassigned transform should not be used directly as IF estimates as the oscillations created either by the interference or the noise on the spectrogram ridge are interpreted as related to the signal. In this regard, we showed that by considering the most significant local modulus maxima along the ridges of the reassigned transforms, it was possible to build new robust IF estimates using very few TF points. In a near future, we would like to find a mean to fully characterize the zeros of the reassignment vector of any order and to better understand the reassignment process of noisy signals so as to find a mean to control the oscillations of the ridges of high order reassigned transforms.

Appendix

A. Proof of Prosposition III.1

Referring to Proposition III.1 of [21], one can write that:

$$r_2^{[3]} = r_2^{[2]} - x_{3,2}r_2^{[3]}. \tag{44}$$

in which $x_{k,1} = \frac{V_f^{t^{k-1}h}}{2i\pi V_f^h}$ and then $x_{k,j} = \frac{\partial_\eta x_{k,j-1}}{\partial_\eta x_{k,j-1}}$ meaning that:

$$x_{3,2} = \frac{\partial_\eta x_{3,1}}{\partial_\eta x_{2,1}} = \frac{\partial_\eta \frac{V_f^{t^2h}}{V_f^h}}{\partial_\eta \frac{V_f^{th}}{V_f^h}} = \frac{V_f^{t^2h}V_f^{th} - V_f^{t^3h}V_f^h}{(V_f^{th})^2 - V_f^{t^2h}V_f^h}$$

As we also have:

$$\begin{aligned}\tilde{\omega}_f^{[3]} &= \tilde{\omega}_f - r_2^{[3]}x_{2,1} - r_3^{[3]}x_{3,1}\\ &= \tilde{\omega}_f^{[2]} + r_3^{[3]}(x_{2,1}x_{3,2} - x_{3,1})\end{aligned}$$

and thus

$$\begin{aligned}\widehat{\omega}_f^{[3]} &= \widehat{\omega}_f^{[2]} + \Re\left\{r_3^{[3]}(x_{2,1}x_{3,2} - x_{3,1})\right\}\\ &= \widehat{\omega}_f^{[2]} + \Im\left\{\frac{r_3^{[3]}}{2\pi}\frac{(V_f^{t^2h})^2 - V_f^{t^3h}V_f^{th}}{(V_f^{th})^2 - V_f^{t^2h}V_f^h}\right\}\\ &= \widehat{\omega}_f^{[2]} + \Im\left\{\frac{r_3^{[3]}}{2\pi}\right\}\Re\left\{\frac{(V_f^{t^2h})^2 - V_f^{t^3h}V_f^{th}}{(V_f^{th})^2 - V_f^{t^2h}V_f^h}\right\}\\ &\quad + \Re\left\{\frac{r_3^{[3]}}{2\pi}\right\}\Im\left\{\frac{(V_f^{t^2h})^2 - V_f^{t^3h}V_f^{th}}{(V_f^{th})^2 - V_f^{t^2h}V_f^h}\right\}\\ &= \widehat{\omega}_f^{[2]} + \Im\left\{\frac{r_3^{[3]}}{2\pi}\right\}\Re\left\{\frac{(V_f^{t^2h})^2 - V_f^{t^3h}V_f^{th}}{(V_f^{th})^2 - V_f^{t^2h}V_f^h}\right\}.\end{aligned} \tag{45}$$

Note that the last equality holds because A is constant.

B. Proof of Proposition IV.1

In the context of Proposition IV.1, the zeros of $\widehat{\omega}_f - \eta$ satisfy:

$$\begin{aligned}&\partial_\eta|V_f^h(t,\eta)|^2 = 0\\ \Leftrightarrow\ & A^2(\eta-\xi_1)e^{-2\pi\sigma^2(\eta-\xi_1)^2} + (\eta-\xi_2)e^{-2\pi\sigma^2(\eta-\xi_2)^2} +\\ & A(2\eta-\xi_1-\xi_2)e^{-\pi\sigma^2\left[(\eta-\xi_1)^2+(\eta-\xi_2)^2\right]}\cos(2\pi(\xi_2-\xi_1)t) = 0.\end{aligned}$$

Then, among these zeros, those satisfying $V_f^hV_f^{t^2h} - (V_f^{th})^2 \neq 0$ are also zeros of $\widehat{\omega}_f^{[2]} - \eta$ if they satisfy:

$$\begin{aligned}&\partial_\eta|V_f^{th}(t,\eta)|^2 = \frac{1}{4\pi^2}\partial_\eta|\partial_\eta V_f^h(t,\eta)|^2\\ &= \sigma^6(2\partial_\eta|V_f^h(t,\eta)|^2 - A^2 4\pi\sigma^2(\eta-\xi_1)^3e^{-2\pi\sigma^2(\eta-\xi_1)^2}\\ &-4\pi\sigma^2(\eta-\xi_2)^3e^{-2\pi\sigma^2(\eta-\xi_2)^2} - 4A\pi\sigma^2(\eta-\xi_1)(\eta-\xi_2)\\ &(2\eta-\xi_1-\xi_2)e^{-\pi\sigma^2\left[(\eta-\xi_1)^2+(\eta-\xi_2)^2\right]}\cos(2\pi(\xi_2-\xi_1)t)) = 0.\end{aligned}$$

Then, from these two equations we get that the zeros of

$\widehat{\omega}_f - \eta$ are zeros of $\widehat{\omega}_f^{[2]} - \eta$ if and only if:

$$\begin{aligned}
-A^2(\eta-\xi_1)^3 e^{-2\pi\sigma^2(\eta-\xi_1)^2} - (\eta-\xi_2)^3 e^{-2\pi\sigma^2(\eta-\xi_2)^2} \\
-A(\eta-\xi_1)(\eta-\xi_2)(2\eta-\xi_1-\xi_2) e^{-\pi\sigma^2\left[(\eta-\xi_1)^2+(\eta-\xi_2)^2\right]} \\
\cos(2\pi(\xi_2-\xi_1)t)) \\
= (\xi_2-\xi_1) \\
\left[-A^2(\eta-\xi_1)^2 e^{-2\pi\sigma^2(\eta-\xi_1)^2} + (\eta-\xi_2)^2 e^{-2\pi\sigma^2(\eta-\xi_2)^2}\right] = 0.
\end{aligned}$$

or equivalently:

$$A(\eta-\xi_1)e^{-\pi\sigma^2(\eta-\xi_1)^2} = \pm(\eta-\xi_2)e^{-\pi\sigma^2(\eta-\xi_2)^2}.$$

C. Proof of Proposition IV.2

Assume $A(\eta-\xi_1)e^{-\pi\sigma^2(\eta-\xi_1)^2} = -(\eta-\xi_2)e^{-\pi\sigma^2(\eta-\xi_1)^2}$, then we may write:

$$\begin{aligned}
\partial_\eta |V_f^h(t,\eta)|^2 = 0 \Leftrightarrow \\
(2\eta-\xi_1-\xi_2)(\eta-\xi_1) \\
(1-\cos(2\pi(\xi_2-\xi_1)t))e^{-2\pi\sigma^2(\eta-\xi_2)^2} = 0 \\
\Leftrightarrow t = t_k = \frac{k}{\xi_2-\xi_1},
\end{aligned} \tag{46}$$

since it can be easily shown that the η of interest are different from ξ_1 and $\frac{\xi_1+\xi_2}{2}$. When $A(\eta-\xi_1)e^{-\pi\sigma^2(\eta-\xi_1)^2} = (\eta-\xi_2)e^{-\pi\sigma^2(\eta-\xi_1)^2}$, we similarly obtain that the time instants t corresponding to the studied zeros are the $\tilde{t}_k = \frac{k+1/2}{\xi_2-\xi_1},\ k \in \mathbb{Z}$.

D. Proof of Proposition IV.3

As one can easily show that $\eta_2^{\max} < \eta_2^{\min}$, and as $|V_f^h(t_k,.)|^2$ attains a maximum at $\eta_2^{\max}$ its derivative is negative on $[\eta_2^{\max}, \eta_2^{\min}]$, which is, using (34), equivalent to:

$$-A(\eta-\xi_1)e^{-\pi\sigma^2(\eta-\xi_1)^2} \leq (\eta-\xi_2)e^{-\pi\sigma^2(\eta-\xi_2)^2}. \tag{47}$$

Similarly, remarking that $|V_f^h(\tilde{t}_k,.)|^2$ attains a maximum at $\eta_2^{\min}$, its derivative is positive on $[\eta_2^{\max}, \eta_2^{\min}]$, meaning that, on that interval

$$-A(\eta-\xi_1)e^{-\pi\sigma^2(\eta-\xi_1)^2} \geq -(\eta-\xi_2)e^{-\pi\sigma^2(\eta-\xi_2)^2} \tag{48}$$

Putting (47) and (48) together, we get that on the interval $[\eta_2^{\max}, \eta_2^{\min}]$:

$$|A(\eta-\xi_1)e^{-\pi\sigma^2(\eta-\xi_1)^2}| \leq |(\eta-\xi_2)e^{-\pi\sigma^2(\eta-\xi_2)^2}|. \tag{49}$$

Then, we remark that on the upper spectrogram ridge, η belongs to $[\eta_2^{\max}, \eta_2^{\min}]$. Using arguments developed in the proof of Proposition IV.1, one can write that at such (t,η), i.e. such that $\partial_\eta |V_f^h(t,\eta)|^2 = 0$, one has:

$$\begin{aligned}
\widehat{\omega}_f^{[2]}(t,\eta) - \eta \\
= \frac{|V_f^h(t,\eta)|^2 \partial_\eta |V_f^{th}(t,\eta)|^2}{|V_f^h(t,\eta)V_f^{t^2h}(t,\eta) - (V_f^{th}(t,\eta))^2|^2} \\
= 4\pi\sigma^8 \frac{|V_f^h(t,\eta)|^2(\xi_2-\xi_1)}{|V_f^h(t,\eta)V_f^{t^2h}(t,\eta) - (V_f^{th}(t,\eta))^2|^2} \\
\left[-A^2(\eta-\xi_1)^2 e^{-2\pi\sigma^2(\eta-\xi_1)^2} + (\eta-\xi_2)^2 e^{-2\pi\sigma^2(\eta-\xi_2)^2}\right],
\end{aligned} \tag{50}$$

which has the sign of $-A^2(\eta-\xi_1)^2 e^{-2\pi\sigma^2(\eta-\xi_1)^2} + (\eta-\xi_2)^2 e^{-2\pi\sigma^2(\eta-\xi_2)^2}$. Using (49), we can thus deduce that the reassignment vector on the upper spectrogram ridge is oriented towards higher frequencies and is null at points $(\tilde{t}_k, \eta_2^{\min})$ and $(t_k, \eta_2^{\max})$.

The same reasoning can be carried out for the lower ridge, namely studying the reassignment vector on the interval $[\eta_0^{\min}, \eta_0^{\max}]$, and enables us to show that the second order reassignment vector on that ridge is oriented towards lower frequencies.

REFERENCES

[1] U. R. Acharya, K. P. Joseph, N. Kannathal, L. C. Min, and J. S. Suri, "Heart rate variability," in *Advances in cardiac signal processing*. Springer, 2007, pp. 121–165.

[2] M. Malik and A. J. Camm, *Dynamic electrocardiography*. John Wiley & Sons, 2008.

[3] M. Costa, A. A. Priplata, L. A. Lipsitz, Z. Wu, N. E. Huang, A. L. Goldberger, and C.-K. Peng, "Noise and poise: Enhancement of postural complexity in the elderly with a stochastic-resonance-based therapy," *Europhysics Letters (EPL)*, vol. 77, no. 6, p. 68008, Mar 2007.

[4] D. A. Cummings, R. A. Irizarry, N. E. Huang, T. P. Endy, A. Nisalak, K. Ungchusak, and D. S. Burke, "Travelling waves in the occurrence of dengue haemorrhagic fever in Thailand," *Nature*, vol. 427, no. 6972, pp. 344 –347, Jan 2004.

[5] C. L. Herry, M. Frasch, A. J. Seely, and H.-T. Wu, "Heart beat classification from single-lead ECG using the synchrosqueezing transform," *Physiological Measurement*, vol. 38, no. 2, pp. 171–187, 2017.

[6] P. Flandrin, *Time-frequency/time-scale analysis*. Academic Press, 1998, vol. 10.

[7] L. Stankovic, M. Dakovic, and V. Ivanovic, "Performance of spectrogram as IF estimator," *Electronics Letters*, vol. 37, no. 12, pp. 797–799, 2001.

[8] R. Carmona, W. Hwang, and B. Torresani, "Multiridge detection and time-frequency reconstruction," *IEEE Transactions on Signal Processing*, vol. 47, no. 2, pp. 480–492, Feb 1999.

[9] T. Oberlin, S. Meignen, and V. Perrier, "The Fourier-based synchrosqueezing transform," in *2014 IEEE International Conference on Acoustics, Speech and Signal Processing (ICASSP)*, May 2014, pp. 315–319.

[10] G. Thakur and H.-T. Wu, "Synchrosqueezing-based recovery of instantaneous frequency from nonuniform samples." *SIAM J. Math. Analysis*, vol. 43, no. 5, pp. 2078–2095, 2011.

[11] I. Daubechies and S. Maes, "A nonlinear squeezing of the continuous wavelet transform based on auditory nerve models," *Wavelets in medicine and biology*, pp. 527–546, 1996.

[12] I. Daubechies, J. Lu, and H.-T. Wu, "Synchrosqueezed wavelet transforms: an empirical mode decomposition-like tool," *Applied and Computational Harmonic Analysis*, vol. 30, no. 2, pp. 243–261, 2011.

[13] G. Yu, T. Lin, Z. Wang, and Y. Li, "Time-reassigned multisynchrosqueezing transform for bearing fault diagnosis of rotating machinery," *IEEE Transactions on Industrial Electronics*, vol. 68, no. 2, pp. 1486–1496, 2020.

[14] C. Li and M. Liang, "Time–frequency signal analysis for gearbox fault diagnosis using a generalized synchrosqueezing transform," *Mechanical Systems and Signal Processing*, vol. 26, pp. 205–217, 2012.

[15] X. Wang, B. Wang, and W. Chen, "The second-order synchrosqueezing continuous wavelet transform and its application in the high-speed-train induced seismic signal," *IEEE Geoscience and Remote Sensing Letters*, 2020.

[16] H.-T. Wu, Y.-H. Chan, Y.-T. Lin, and Y.-H. Yeh, "Using synchrosqueezing transform to discover breathing dynamics from ecg signals," *Applied and Computational Harmonic Analysis*, vol. 36, no. 2, pp. 354–359, 2014.

[17] H.-t. Wu, R. Talmon, and Y.-L. Lo, "Assess sleep stage by modern signal processing techniques," *IEEE Transactions on Biomedical Engineering*, vol. 62, no. 4, pp. 1159–1168, 2014.

[18] J. M. Miramont, M. A. Colominas, and G. Schlotthauer, "Voice jitter estimation using high-order synchrosqueezing operators," *IEEE/ACM Transactions on Audio, Speech, and Language Processing*, 2020.

[19] R. Behera, S. Meignen, and T. Oberlin, "Theoretical analysis of the second-order synchrosqueezing transform," *Applied and Computational Harmonic Analysis*, vol. 45, no. 2, pp. 379–404, 2018.

[20] T. Oberlin, S. Meignen, and V. Perrier, "Second-order synchrosqueezing transform or invertible reassignment? Towards ideal time-frequency representations," *IEEE Transactions on Signal Processing*, vol. 63, no. 5, pp. 1335–1344, March 2015.

[21] D. H. Pham and S. Meignen, "High-order synchrosqueezing transform for multicomponent signals analysis-with an application to gravitational-wave signal." *IEEE Trans. Signal Processing*, vol. 65, no. 12, pp. 3168–3178, 2017.

[22] X. Zhu, Z. Zhang, J. Gao, and W. Li, "Two robust approaches to multicomponent signal reconstruction from STFT ridges," *Mechanical Systems and Signal Processing*, vol. 115, pp. 720–735, 2019.

[23] L. Li, H. Cai, and Q. Jiang, "Adaptive synchrosqueezing transform with a time-varying parameter for non-stationary signal separation," *Applied and Computational Harmonic Analysis*, 2019.

[24] L. Li, H. Cai, H. Han, Q. Jiang, and H. Ji, "Adaptive short-time Fourier transform and synchrosqueezing transform for non-stationary signal separation," *Signal Processing*, vol. 166, p. 107231, 2020.

[25] V. Bruni, M. Tartaglione, and D. Vitulano, "On the time-frequency reassignment of interfering modes in multicomponent FM signals," in *2018 26th European Signal Processing Conference (EUSIPCO)*. IEEE, 2018, pp. 722–726.

[26] ——, "A fast and robust spectrogram reassignment method," *Mathematics*, vol. 7, no. 4, p. 358, 2019.

[27] R. G. Baraniuk, P. Flandrin, A. J. Janssen, and O. J. Michel, "Measuring time-frequency information content using the Rényi entropies," *IEEE Transactions on Information theory*, vol. 47, no. 4, pp. 1391–1409, 2001.

[28] A. Berrian and N. Saito, "Adaptive synchrosqueezing based on a quilted short-time fourier transform," in *Wavelets and Sparsity XVII*, vol. 10394. International Society for Optics and Photonics, 2017, p. 1039420.

[29] S. Meignen, M. Colominas, and D.-H. Pham, "On the use of Rényi entropy for optimal window size computation in the short-time Fourier transform," in *ICASSP 2020-2020 IEEE International Conference on Acoustics, Speech and Signal Processing (ICASSP)*. IEEE, 2020, pp. 5830–5834.

[30] R. Carmona, W. Hwang, and B. Torresani, "Characterization of signals by the ridges of their wavelet transforms," *IEEE Transactions on Signal Processing*, vol. 45, no. 10, pp. 2586–2590, Oct 1997.

[31] N. Laurent and S. Meignen, "A novel ridge detector for nonstationary multicomponent signals: Development and application to robust mode retrieval," *IEEE Transactions of Signal Processing*, vol. doi:10.1109/TSP.2021.3085113, 2021.